



# Exosomes isolated from melatonin-stimulated mesenchymal stem cells improve kidney function by regulating inflammation and fibrosis in a chronic kidney disease mouse model

Ji-Hye Yea<sup>1</sup> , Yeo Min Yoon<sup>1</sup>, Jun Hee Lee<sup>2,3,4,5</sup>, Chul Won Yun<sup>1</sup> and Sang Hun Lee<sup>1,6,7,8</sup>

## Abstract

Chronic kidney disease (CKD) is defined as structural and functional abnormalities of the kidney due to inflammation and fibrosis. We investigated the therapeutic effects of exosomes secreted by melatonin-stimulated mesenchymal stem cells (Exocue) on the functional recovery of the kidney in a CKD mouse model. Exocue upregulated gene expression of micro RNAs (miRNAs) associated with anti-inflammatory and anti-fibrotic effects. Exocue-treated groups exhibited low tumor necrosis factor- $\alpha$  and transforming growth factor- $\beta$  levels in serum and fibrosis inhibition in kidney tissues mediated through regulation of cell apoptosis and proliferation of fibrosis-related cells. Exocue treatment decreased the gene expression of CKD progression-related miRNAs. Moreover, the CKD severity was alleviated in the Exocue group via upregulation of aquaporin 2 and 5 levels and reduction of blood urea nitrogen and creatinine, resulting in functional recovery of the kidney. In conclusion, Exocue could be a novel therapeutic agent for treating CKD by regulating inflammation and fibrosis.

## Keywords

Chronic kidney disease, mesenchymal stem cell, exosome, inflammation, fibrosis

Date received: 17 August 2021; accepted: 25 October 2021

## Introduction

Chronic kidney disease (CKD) is defined based on the presence of structural and functional abnormalities of the kidney with a decreased glomerular filtration rate for >3 months.<sup>1</sup> In the US, the prevalence of CKD is high at 8%–16% with an associated costs of almost \$23 billion, representing 6.4% of the entire Medicare budget.<sup>2</sup> Although structural and functional problems of the kidney are the main cause of CKD, the present therapeutic strategies target blood pressure, blood sugar, and dyslipidemia, which does not address the fundamental etiology such as inflammation and fibrosis. Although kidney transplantation is the best option for enhancing kidney function, there are critical limitations to finding a suitable donor.<sup>3</sup> Thus, it is crucial to find new therapeutic strategies to treat CKD that solve the structural problems and dysfunction of the damaged kidney.

<sup>1</sup>Medical Science Research Institute, Soonchunhyang University Seoul Hospital, Seoul, Republic of Korea

<sup>2</sup>Institute of Tissue Regeneration Engineering, Dankook University, Cheonan, Republic of Korea

<sup>3</sup>Department of Nanobiomedical Science and BK21 PLUS NBM Global Research Center for Regenerative Medicine, Dankook University, Cheonan, Republic of Korea

<sup>4</sup>Department of Oral Anatomy, College of Dentistry, Dankook University, Cheonan, Republic of Korea

<sup>5</sup>Cell and Matter Institute, Dankook University, Cheonan, Republic of Korea

<sup>6</sup>Department of Biochemistry, Soonchunhyang University College of Medicine, Cheonan, Republic of Korea

<sup>7</sup>Department of Biochemistry, BK21FOUR Project2, College of Medicine, Soonchunhyang University, Cheonan, Republic of Korea

<sup>8</sup>StemBio Ltd., Asan, Republic of Korea

## Corresponding author:

Sang Hun Lee, Soonchunhyang Medical Science Research Institute, Soonchunhyang University Seoul Hospital, 59, Daesagwan-ro (657 Hannam-dong), Yongsan-gu, Seoul 04401, Republic of Korea.  
Email: shlee0551@gmail.com



Mesenchymal stem cells (MSCs) have emerged as a promising therapeutic strategy in regenerative medicine.<sup>4</sup> MSCs isolated from various tissues such as the bone marrow (BM), adipose (AD), muscle, and umbilical cord (UC), have the ability to differentiate into various cells such as osteocytes, endothelial cells, and chondrocytes.<sup>5,6</sup> The paracrine effect of MSCs is also known to not only induce tissue regeneration without fibrosis, but also to inhibit inflammation.<sup>4,6,7</sup> However, the use of MSCs is associated with some risks because they can induce immune rejection responses and differentiate into cells other than those intended, especially tumor cells.<sup>7,8</sup> Moreover, the engraftment rate of cells after MSC transplantation is low.<sup>9</sup> Therefore, another promising approach using MSCs is required to overcome these drawbacks.

Recent studies to determine the therapeutic effect of stem cells and to avoid the risk factors of MSC transplantation have focused on cell-derived substances such as exosomes. Exosomes are 50–200 nm soluble microvesicles with a bi-lipid membrane that are secreted by various cells.<sup>10</sup> Exosomes released from MSCs have anti-apoptotic, anti-inflammatory, and anti-oxidant effects, which are paracrine effects of origin-MSCs.<sup>11</sup> Previous studies have reported that exosomes derived from MSCs modulate the behavior of epithelial cells in kidney disease, migration of inflammatory cells in uveitis, and fibrosis of hepatic cells in liver failure through the delivery of various bioactive factors such as specific proteins, mRNA, and microRNA (miRNA), which they contained.<sup>12–14</sup> Moreover, the application of exosomes is safe for clinical use because exosomes do not remain at the sites of injection or/and injury whereas MSCs settle at the site of injury.<sup>15</sup> These findings suggest that exosomes could be potential therapeutic agents for translational applications using stem cells.

To enhance the efficacy of exosomes, origin cells have been biologically engineered using various stimuli such as pro-inflammatory, growth, and transcription factors and mechanical stimulation in the cell engineering field.<sup>16</sup> Melatonin, an endogenous hormone mainly produced and excreted by the pineal gland, is one of these stimulus options.<sup>17,18</sup> Melatonin plays crucial roles in immunoregulatory activities by suppressing apoptotic and necrotic changes and infiltration of inflammatory cells, and by preventing tissue fibrosis after injury through inhibition of fibrogenic effects in injured cells.<sup>19</sup> Recent studies have demonstrated that stimulation with melatonin enhanced the efficacy of stem cells in some diseases such as myocardial infarction, ischemic kidney, acute lung ischemia-reperfusion injury, and hindlimb ischemia.<sup>20–25</sup>

However, there are no reports on the efficacy of exosomes derived from MSCs stimulated by melatonin on inflammation and fibrosis as well as kidney function in CKD. Therefore, in this study, we hypothesized that exosomes from melatonin-stimulated MSCs (Exocue)

could improve kidney function by modulating inflammation and fibrosis in CKD, which we investigated by determining their suppression of inflammation and fibrosis in a CKD mouse model.

## Materials and methods

### Isolation of MSC-derived exosomes

Human AD-derived MSCs were purchased from Sigma-Aldrich (SCC038; St-Louis, MO, USA). The MSCs were cultured in  $\alpha$ -minimum essential medium (MEM; Thermo Fisher Scientific, Waltham, MA, USA) supplemented with 10% fetal bovine serum (FBS; Thermo Fisher Scientific) and antibiotic solution (100 U/mL penicillin; Thermo Fisher Scientific) in a 5% CO<sub>2</sub> incubator with humidified air at 37°C. When the cells reached 60%–80% confluence, they were treated with or without melatonin (1  $\mu$ M/mL) in serum-free medium, which was harvested after 24 h (the dose of melatonin was decided according to our previous study<sup>3</sup>). Exosomes were extracted from the medium using an exosome isolation kit (Rosetta Exosome, Seongnam, Korea) and concentrated using centrifugal filters (Millipore, Burlington, MA, USA). Exosomes isolated from naïve MSCs treated without and with melatonin were used as control exosomes (cExo) and the Exocue groups, respectively.

### miRNA microarray

miRNA profiling was performed and the data consisting of 1100 known human miRNAs were analyzed by Komabiotech (Seoul, Korea) using Affymetrix miRNA microarrays (Affymetrix Inc., Santa Clara, CA, USA). At least three exosome samples were used in the experiments. The signals were scaled to a median array intensity of 100 using GCOS 1.2 to compare different arrays and Spotfire DecisionSite 8.2 ([www.spotfire.com](http://www.spotfire.com)) was used for gene profiling analysis.<sup>3</sup>

### Nanoparticle tracking analysis (NTA)

We measured the diameter and concentration of each exosome using a NanoSight LM10-HS system (Malvern Instruments Ltd., Malvern, UK) with a 688 nm laser. Exosomes (10  $\mu$ L) were diluted 1:100 in phosphate-buffered saline (PBS). The size of the exosomes in solution were evaluated using zeta potential and particle size analysis and the data were analyzed using NTA software version 2.3 (Malvern Instrument Ltd.).

### Cryo-electron microscopy (EM)

Exosomes were absorbed onto 300-mesh electron microscopy (EM) carbon grids with a hydrophilic surface and

frozen using Vitrobot (Thermo Fisher Scientific) in liquid nitrogen. The grids were examined and analyzed using a Talos L120C cryo-transmission EM (TEM, Thermo Fisher Scientific). We observed and recorded the images using light microscopy at 13,000 magnification.

### Western blot analysis

Protein extracts of exosomes were separated using 10%–15% sodium dodecyl sulfate-polyacrylamide gel electrophoresis (SDS-PAGE) and the proteins were transferred onto a 0.2  $\mu$ m PVDF membrane. The membranes were blocked in 3% skim milk for 1 h and then incubated overnight with primary antibodies against CD81 and CD9 (both 1:1000; Santa Cruz Biotechnology, Dallas, TX, USA) at 4°C. After washing twice with Tris-buffered saline plus Tween (TBST), the membrane was incubated with goat anti-rabbit IgG or goat anti-mouse IgG secondary antibodies (Abcam, Cambridge, UK). The blots were subsequently developed using enhanced chemiluminescence (GE Healthcare, Chicago, IL, USA).

### In vivo study design

All animal procedures were conducted in accordance with the protocol approved by the Institutional Animal Care and Use Committee of Soonchunhyang University Seoul Hospital (IACUC-SCH-2020-08) and in accordance with the National Research Council (NRC) Guidelines for the Care and Use of Laboratory Animals. Six-week-old male BALB/c mice (Biogenomics, Seoul, Korea) were maintained under a 12-h light/dark cycle at 25°C. The mice were randomly divided into the following five groups ( $n=5$  each): (1) healthy, (2) PBS-treated CKD, (3) cExo-treated CKD, (4) 50  $\mu$ g Exocue-treated CKD, and (5) 100  $\mu$ g Exocue-treated CKD groups.

Mice in the CKD groups were fed a 0.25% adenine-containing diet to induce CKD. After 1 week, the mice were injected with PBS, cExo (100  $\mu$ g), or Exocue (50 or 100  $\mu$ g) through the tail vein twice a week for 2 weeks. During the experimental period all the mice were fed a normal diet and 3 weeks after administration, cortical kidney tissue and blood were harvested from the mice. Left kidney tissue samples were histologically evaluated, and the right kidney tissue samples were divided into two parts for enzyme-linked immunosorbent assay (ELISA) and quantitative reverse transcription-polymerase chain reaction (qRT-PCR).

### Concentration of protein in cortical kidney and serum of CKD mouse model

Collected blood was centrifuged at 1500 rpm for 30 min and the upper layer was collected as the serum, which was evaluated for levels of tumor necrosis factor (TNF)- $\alpha$ ,

transforming growth factor (TGF)- $\beta$ , blood urea nitrogen (BUN), and creatinine. Harvested cortical kidney tissues were lysed with radioimmunoprecipitation assay (RIPA) buffer (CUREBIO, Seoul, Korea) and the aquaporin 2 (AQP2) and AQP5 levels were measured. A quantitative sandwich enzyme immunoassay was used to measure the serum concentrations of TNF- $\alpha$ , TGF- $\beta$ , BUN, and creatinine and the concentrations of AQP2 and AQP5 in kidney tissues. The protein concentration used was 50  $\mu$ g in all experiments. Immunoassays were performed using an ELISA kit (Komabiotech, Seoul, Korea) according to the manufacturer's instructions. The optical densities of the microplate wells were evaluated by measuring the absorbance using a microplate reader (Thermo Fisher Scientific) at a wavelength of 450 nm.

### Immunohistochemical, Masson's trichrome (MT), and Picro Sirius red (PSR) staining

Cortical kidney tissue samples were collected, immediately fixed with 4% paraformaldehyde (CureBio, Seoul, Korea), and then embedded in paraffin. For histological analysis, the kidney tissue samples were stained with Masson's trichrome (MT) or Picro Sirius red (PSR) to determine the presence of fibrosis and the stained tissues were examined using light microscopy (U-TVO 63XC; Olympus Corp., Tokyo, Japan). The MT and PSR stained area were measured using Image J software with installed NII plugin (National Institutes of Health, MD, USA).<sup>4</sup>

Immunofluorescence staining was also performed with primary antibodies against cleaved caspase 3 (Novus Biologicals, Denver, CO, USA), proliferating cell nuclear antigen (PCNA, Abcam), and  $\alpha$ -smooth muscle actin (SMA; Santa Cruz Biotechnology), followed by secondary antibodies conjugated with Alexa Fluor 488 or 594 (Thermo Fisher Scientific). The nuclei were stained with 4,6-diaminido-2-phenylindol (DAPI, Sigma-Aldrich), and the immunostained samples were examined using a confocal microscope (Olympus, Tokyo, Japan). The apoptosis (or proliferation) index was determined as number of caspase-3 (or PCNA) positive cells/total number of cells  $\times$  100.<sup>26</sup>

### Quantification of miRNA

Total RNA was extracted from the harvested cortical kidney tissues (DNase digested) using mirVana (Thermo Fisher Scientific) and miRNAs were synthesized for cDNA with A-tailing using an miRNA cDNA synthesis kit (ABM, Richmond, BC, Canada). The qRT-PCR (Applied Biosystems, Waltham, MA, USA) was performed using a SYBR Green Master Mix (Thermo Fisher Scientific). The gene expression levels of *miR-4270*, *miR-4739*, *miR-636*, *miR-320c*, *miR-572*, TGF- $\beta$ , nuclear factor-kappa B (NF- $\kappa$ B), insulin-like growth factor-1 (IGF-1), and connective

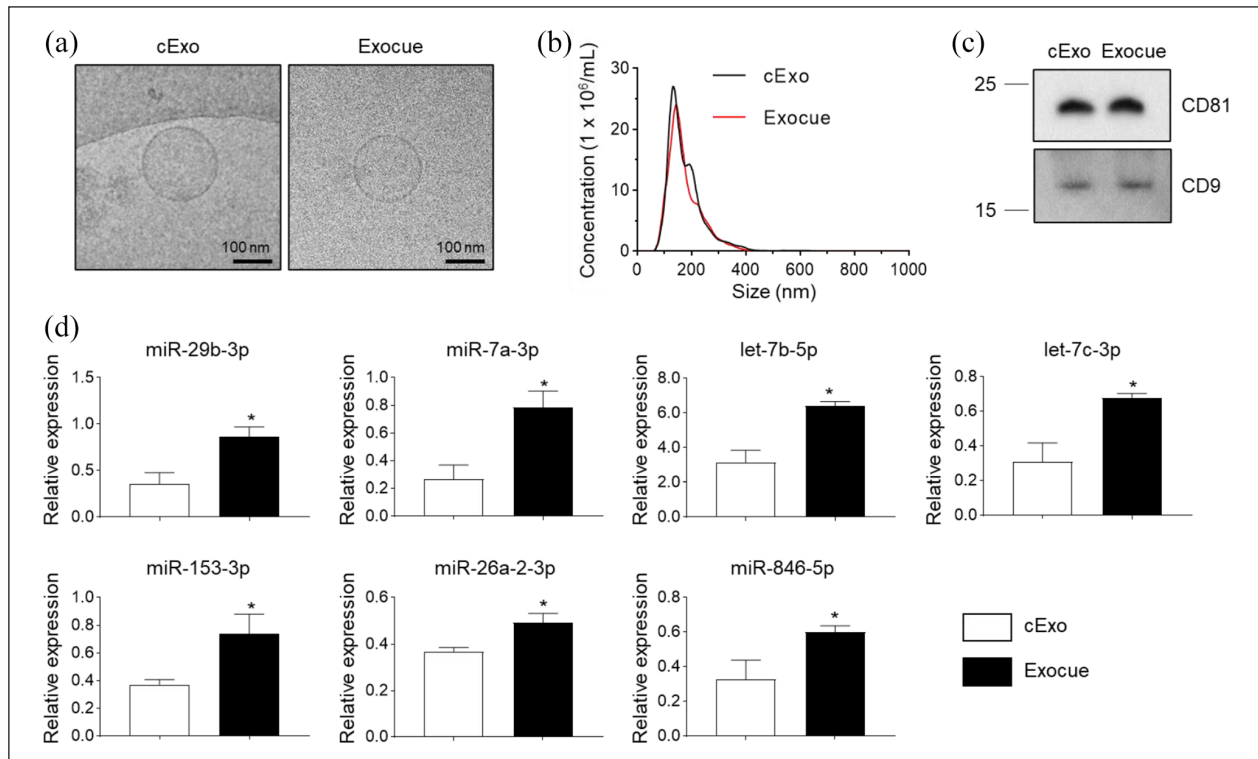


**Figure 1.** Characterization of control exomes (cExo) and exosomes from melatonin-stimulated mesenchymal stem cells (MSCs, Exocue) isolated from MSCs. (a) Representative cryo-electron microscopy images of exosomes (scale bar = 100 nm). (b) Size distribution of cExo and Exocue measured using nanoparticle tracking analysis. (c) Western blot analysis of extracellular vesicle marker proteins CD81 and CD9 in cExo and Exocue. (d) Expression levels of miR-29b-3p, let-7a-3p, let-7b-5p, let-7c-3p, miR-153-3p, miR-26a-2-3p, and miR-846-5p in cExo and Exocue measured using micro RNA (miRNA) microarray. Values represent mean  $\pm$  standard error of the mean (SEM). \* $p < 0.05$ . cExo: control exosome; Exocue: exosome from melatonin-stimulated MSCs; MSCs: mesenchymal stem cells.

tissue growth factor (CTGF) were evaluated and then normalized to that of  $\beta$ -actin.

### Statistical analysis

Two-tailed Student's *t*-test and one- or two-way analysis of variance were used to determine the significant differences among groups, and the results are expressed as the means and standard error of the mean (SEM). Three or more groups were compared using Dunnett's or Tukey's post hoc test and the data were considered significantly different at  $p < 0.05$ .

## Results

### Characterization of MSC-derived exosomes

The TEM image showed that both cExo and Exocue had a spherical nanovesicular morphology without noticeable damage (Figure 1(a)). The nanoparticle tracking analysis showed that the sizes of the cExo and Exocue particles ranged from 50 to 400 nm with an average of  $173.02 \pm 2.34$  and  $177.18 \pm 2.84$  nm, respectively (Figure 1(b)).

Western blotting showed that cExo and Exocue expressed CD81 and CD9, which are extracellular vesicle (EV) markers derived from MSCs (Figure 1(c)). In our previous study, we found that melatonin regulated the expression of miRNAs in exosomes isolated from MSCs.<sup>3</sup> The analysis of miRNA expression in the Exocue group showed that levels of the anti-inflammatory and anti-fibrotic miR-29b-3p, miR-7a-3p, let-7b-5p, let-7c-3p, miR-153-3p, miR-26a-2-3p, and miR-846-5p were upregulated by 2.42-, 2.95-, 2.20-, 2.03-, 1.98-, 1.34-, and 1.84-fold, respectively, compared to levels in the cExo group (Figure 1(d)). These results indicate that while melatonin stimulation increased anti-inflammation and anti-fibrosis-related miRNA expression in exosomes isolated from MSCs, it did not alter the characteristics of EVs isolated from MSCs.

### Exocue decreased inflammation and fibrosis related genes in kidney after CKD

After CKD injury, gene expressions related inflammation and fibrosis such as TGF- $\beta$ , NF- $\kappa$ B, IGF-1, and CTGF were upregulated. After exosomes treated, TGF- $\beta$  and

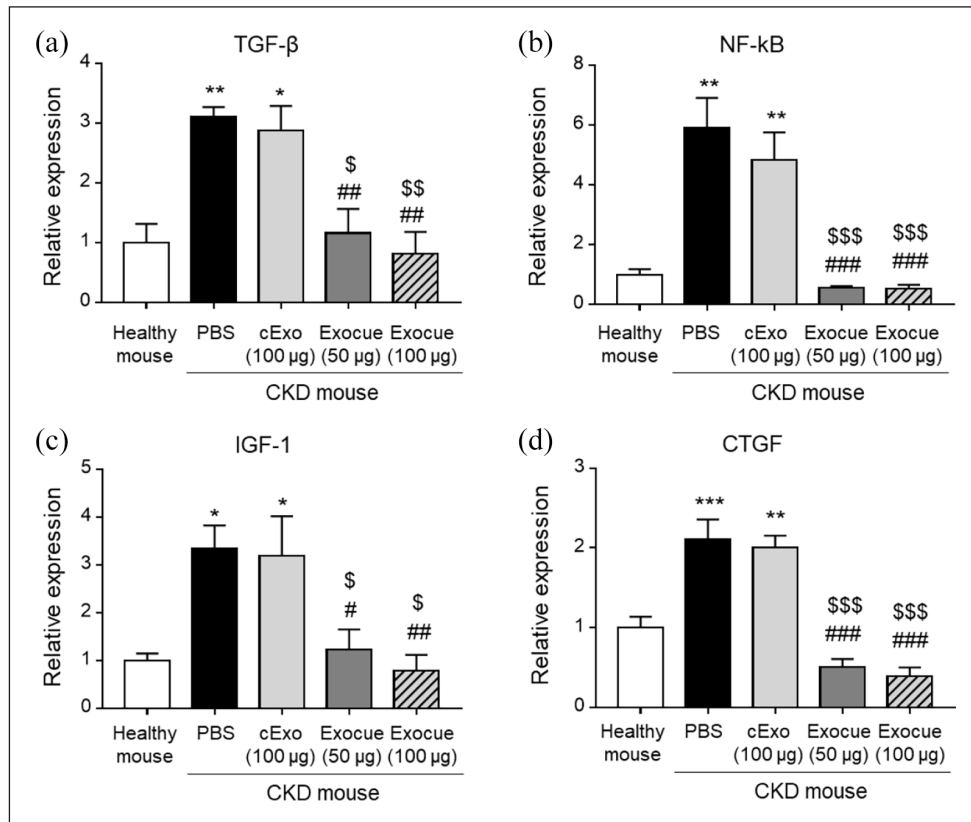


**Figure 2.** Effect of control exomes (cExo), exosomes from melatonin-stimulated mesenchymal stem cells (MSCs, Exocue), and phosphate-buffered saline (PBS) on expression levels of inflammation and fibrosis related genes of kidney tissues 3 weeks after injection in CKD mouse model. (a–d) Expression of TGF- $\beta$ , NF-kB, IGF-1, and CTGF in kidney tissue measured using quantitative reverse transcription-polymerase chain reaction (qRT-PCR). Values represent means  $\pm$  standard error of the means (SEM). \* $p < 0.05$ , \*\* $p < 0.01$ , and \*\*\* $p < 0.001$  versus healthy mice; # $p < 0.05$ , ## $p < 0.01$ , and ### $p < 0.001$  versus PBS; and \$ $p < 0.05$ , \$\$ $p < 0.01$ , and \$\$\$ $p < 0.001$  versus cExo. cExo, control exosome; CKD: chronic kidney disease; CTGF: connective tissue growth factor; Exocue: exosome from melatonin-stimulated MSCs; IGF-1: insulin-like growth factor-1; NF-kB: nuclear factor-kappa B; TGF- $\beta$ : transforming growth factor- $\beta$ .

NF-kB genes were downregulated in Exocue (50  $\mu$ g) group by 0.37- and 0.09-fold and in Exocue (100  $\mu$ g) group by 0.26- and 0.09-fold respectively whereas the genes were not downregulated in cExo group (Figure 2(a) and (b)). Moreover, IGF-1 and CTGF genes were also suppressed in Exocue (50  $\mu$ g) by 0.36- and 0.25-fold and in Exocue (100  $\mu$ g) group by 0.23- and 0.21-fold respectively meanwhile the genes were not changed in cExo group (Figure 2(c) and (d)). These results showed that melatonin-stimulated MSCs secreted EVs, which modulated inflammation and fibrosis related genes under CKD conditions.

### Exocue decreased inflammatory cytokine levels in kidney after CKD

In CKD, uremic toxins accumulate in the blood, inducing inflammation of kidney tissues. The established CKD mouse model exhibited increased levels of pro-inflammatory cytokines such as TNF- $\alpha$  and TGF- $\beta$  (Figure 3(a) and (b)). However, cExo and Exocue (100  $\mu$ g each)

downregulated the synthesis of TNF- $\alpha$  by 0.86- and 0.81-fold, respectively. Furthermore, the Exocue (100  $\mu$ g) group showed a 1.52-fold suppression of TGF- $\beta$  compared to that in the PBS group, whereas cExo did not affect the synthesis of TGF- $\beta$  (Figure 3(a) and (b)). These results showed that melatonin-stimulated MSCs secreted EVs, which modulated pre-inflammatory cytokines such as TNF- $\alpha$  and TGF- $\beta$  under CKD conditions.

### Exocue inhibited apoptosis in the kidney tissues and suppressed fibrotic cell proliferation

To investigate the protective effect of Exocue on kidney tissues in CKD, we assessed the apoptosis of kidney tissue cells in the established murine CKD model after treatment with Exocue. Although the PBS group showed increased caspase-3 stained cells indicating the apoptosis of kidney cells, the cExo group exhibited fewer caspase-3 stained cells (0.44-fold) than that of the PBS group. Moreover, the Exocue (100  $\mu$ g) group showed greater reduction of

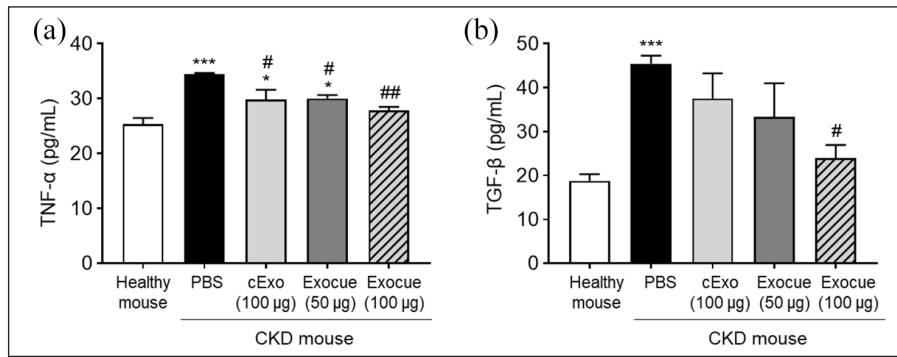


**Figure 3.** Effect of control exosome (cExo) and exosomes from melatonin-stimulated mesenchymal stem cells (MSCs, Exocue) on inflammatory cytokines in blood at 3 weeks after phosphate-buffered saline (PBS) injection in a chronic kidney disease (CKD) mouse model. (a and b) Concentration of TNF- $\alpha$  and TGF- $\beta$  in serum from a CKD mouse model measured using enzyme-linked immunosorbent assay (ELISA). Values represent means  $\pm$  standard error of the mean (SEM). \* $p < 0.05$ , \*\* $p < 0.01$ , and \*\*\* $p < 0.001$  versus healthy mouse and # $p < 0.05$ , ## $p < 0.01$  versus PBS. cExo: control exosome; Exocue: exosome from melatonin-stimulated MSCs; PBS: phosphate-buffered saline; CKD: chronic kidney disease; TNF- $\alpha$ : tumor necrosis factor- $\alpha$ ; TGF- $\beta$ : transforming growth factor- $\beta$ .

caspace-3 stained cells than that of the cExo group (0.44-fold). In particular, the effect was dose-dependent with the 100  $\mu$ g Exocue group having a significantly fewer caspace-3 stained cells (0.60-fold) than that of the 50  $\mu$ g Exocue group (Figure 4(a) and (c)).

To further explore whether Exocue suppresses the proliferation of fibrosis-related cells, we performed immunofluorescence staining for PCNA and  $\alpha$ -SMA in kidney tissues of the Exocue-treated CKD murine model. Immunofluorescence staining showed that PCNA expression in the  $\alpha$ -SMA-positive area was higher in the PBS-treated group than healthy mouse which mean that CKD increased proliferative ability of fibrosis-related cells. However, the PCNA positive cells was reduced in cExo group (0.70-fold) compared to the PBS group. Moreover, the Exocue (100  $\mu$ g) group had fewer PCNA positive cells than that of the cExo group (0.66-fold). Additionally, the effect was dose-dependent with the 100  $\mu$ g Exocue group showing a significantly fewer PCNA stained cells (0.76-fold) than that of the 50  $\mu$ g Exocue group (Figure 4(b) and (d)). These results suggest that Exocue protected kidney tissue against CKD by inhibiting the apoptosis of resident cells and suppressing the proliferation of fibrosis-related cells.

### Exocue protects kidney tissues against CKD-induced fibrosis

In CKD, accumulated uremic toxins in the blood induce fibrosis of kidney tissues, leading to kidney dysfunction. MT and PSR staining of kidney tissue from the established CKD murine model treated with PBS showed severe deposition of collagen, which is related to fibrosis (blue and red in the MT- and PSR-stained images, respectively indicated fibrotic tissues; Figure 5). However, the cExo group

showed smaller area stained by MT and PSR (0.55- and 0.54-fold, respectively) than that of the PBS group. Furthermore, the Exocue (100  $\mu$ g) group showed greater reduction of MT and PSR stained area than that of the cExo group (0.39 and 0.38-fold, respectively). In particular, the effect was dose-dependent with the 100  $\mu$ g Exocue group showing a significantly smaller MT and PSR stained area (0.65- and 0.56-fold, respectively) than that of the 50  $\mu$ g Exocue group (Figure 5). These results suggest that Exocue modulated fibrosis through the inhibition of collagen deposition in CKD.

### Exocue modulated CKD-related gene expression in kidney tissues

A previous study showed that expression levels of miR-4270, miR-4739, miR-636, miR-320c, and miR-572 in kidney tissues are related to CKD.<sup>27</sup> To explore how Exocue protects against CKD, related miRNA expression levels were analyzed in kidney tissues of the CKD mouse model using qPCR. After inducing CKD, the expression levels of related miRNA such as miR-4270, miR-4739, miR-636, miR-320c, and miR-572 were significantly upregulated in the PBS-treated group of CKD mice (Figure 6(a)–(e)). Although cExo treatment did not significantly reduce gene expression, Exocue significantly downregulated the expression of miR-4270, miR-4739, miR-320c, and miR-572 by 0.36-, 0.08-, 0.69-, and 0.37-fold, respectively, compared to those in the PBS group (Figure 6(a)–(e)). Moreover, compared to the cExo group, the gene expression level of miR-4270, miR-4739, and miR-572 in the Exocue group was lower by 0.36-, 0.12-, and 0.45-fold, respectively (Figures 6(e) and 56). These data showed that Exocue could inhibit the gene expression of miRNAs correlated with the severity of CKD in kidney tissues.

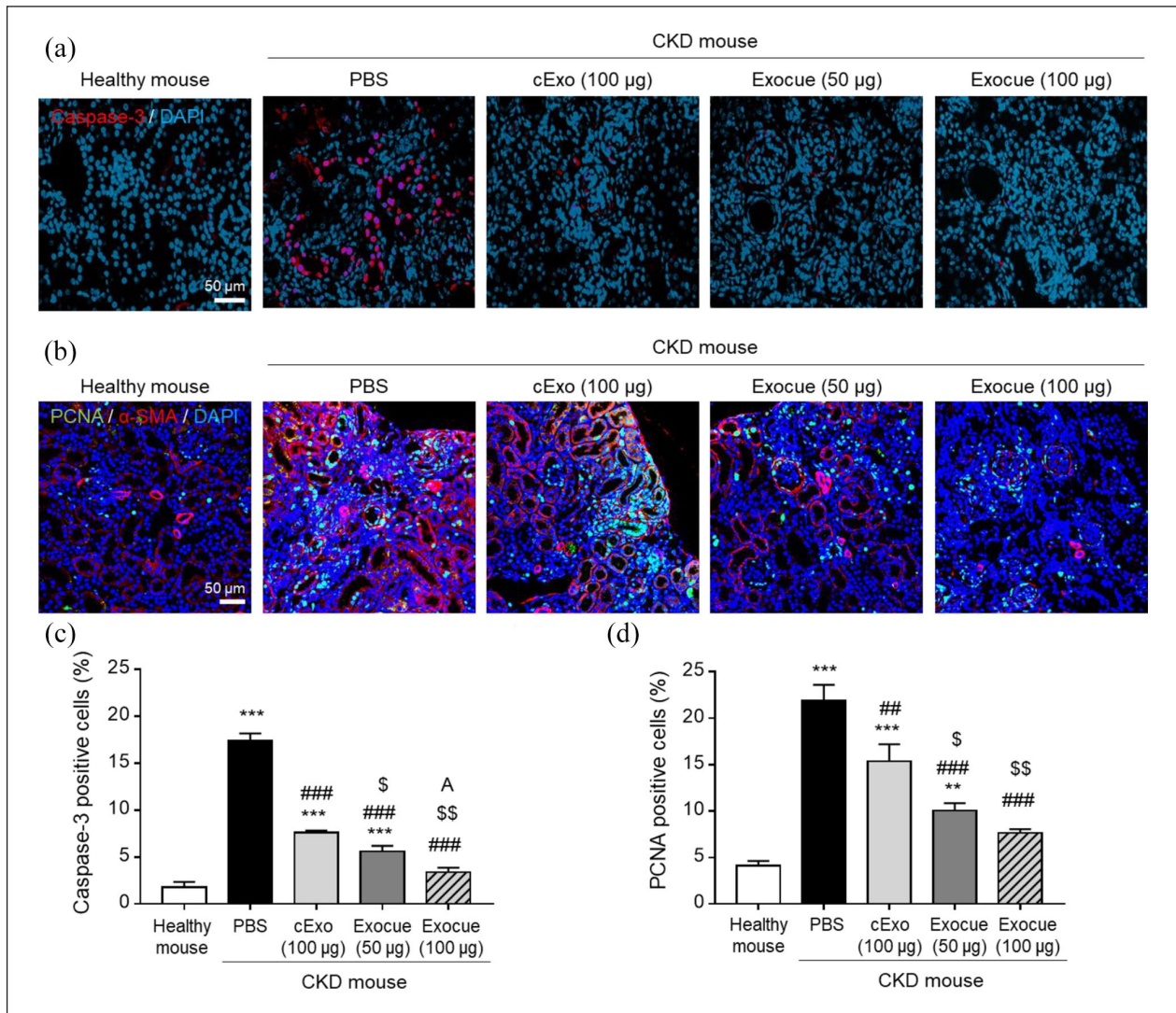


**Figure 4.** Effect of control exosomes (cExo), exosomes from melatonin-stimulated mesenchymal stem cells (MSCs, Exocue), and phosphate-buffered saline (PBS) on suppression of apoptosis, proliferation, and fibrosis of resident kidney cells 3 weeks after injection in a chronic kidney disease (CKD) mouse model. (a) Images of caspase 3- and (b) PCNA- and  $\alpha$ -SMA-stained kidney tissues. (c) Caspase-3 positive cells and (d) PCNA positive cells in the kidney tissues. cExo: control exosome; CKD: chronic kidney disease; Exocue: exosome from melatonin-stimulated MSCs; PCNA: proliferating cell nuclear antigen;  $\alpha$ -SMA: alpha-smooth muscle actin. Values represent means  $\pm$  standard error of the means (SEM). \*\* $p < 0.01$ , and \*\*\* $p < 0.001$  versus healthy mice; ## $p < 0.01$ , and ### $p < 0.001$  versus PBS; \$ $p < 0.05$ , \$\$ $p < 0.01$  versus cExo; and A $p < 0.05$  versus Exocue (50  $\mu$ g).

### Exocue improved kidney function in CKD model

Tissues of CKD mice showed decreased protein synthesis of AQP2 and AQP5, which are water absorption-related proteins,<sup>28,29</sup> whereas accumulation of these proteins was increased following treatment with cExo. However, the Exocue group showed 1.30- and 1.33-fold higher concentrations of AQP2 and AQP5 proteins, respectively than the cExo group did and there were significant differences in the concentration of AQP5 between both groups (Figure 7(a) and (b)). The serum concentrations of BUN and creatinine were significantly increased in the PBS group of CKD mice. After cExo treatment, the BUN concentration was significantly lower by 0.62 than that of the PBS group,

but the creatinine concentration was still increased to a comparable level to that of the PBS group.

However, concentrations of BUN and creatinine in the cExo group were significantly lower (0.23 and 0.33 times, respectively) than those in the PBS group were. Moreover, the Exocue (100  $\mu$ g) group showed lower concentrations of both BUN and creatinine (0.37- and 0.36-fold, respectively), than those of the cExo group. In particular, the effect was dose-dependent with the 100  $\mu$ g Exocue group showing a significantly higher inhibition of BUN protein accumulation (0.59-fold) than that of the 50  $\mu$ g Exocue group (Figure 7(c) and (d)). These results showed that Exocue could improve kidney function through water absorption and filtration of BUN and creatinine in CKD conditions.

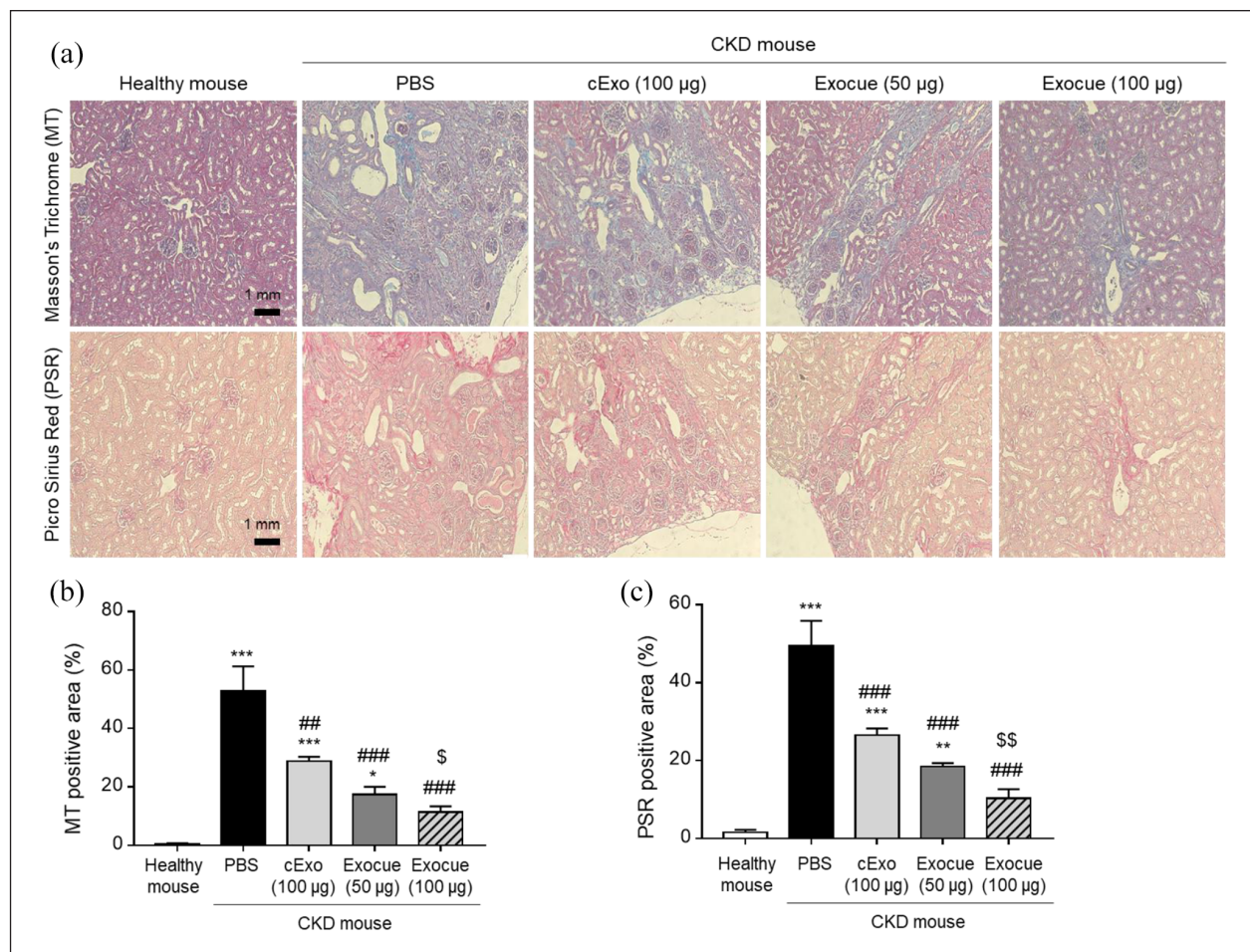


**Figure 5.** Effect of control exomes (cExo), exosomes from melatonin-stimulated mesenchymal stem cells (MSCs, Exocue), and phosphate-buffered saline (PBS) injection on fibrosis of kidney tissues after 3 weeks in chronic kidney disease (CKD) mouse model. (a) Images of MT and PSR staining of kidney tissues. (b) MT positive area and (c) PSR positive area in the kidney tissues. cExo: control exosome; CKD: chronic kidney disease; Exocue: exosome from melatonin-stimulated MSCs; MT: Masson's trichrome; PSR: Picro Sirius red. Values represent means  $\pm$  standard error of the means (SEM). \* $p < 0.05$ , \*\* $p < 0.01$ , and \*\*\* $p < 0.001$  versus healthy mice; ### $p < 0.01$ , and ### $p < 0.001$  versus PBS; and \$ $p < 0.05$ , \$\$ $p < 0.01$  versus cExo.

## Discussion

Following are the findings of this study. (1) MSCs treated with melatonin secreted exosomes with significantly upregulated gene expression of miRNAs such as miR-29b-3p, miR-7a-3p, let-7b-5p, let-7c-3p, miR-153-3p, miR-26a-2-3p, and miR-846-5p, whereas melatonin stimulation did not damage their characteristic EVs. (2) Exosomes derived from melatonin-treated MSCs, Exocue, suppressed inflammatory cytokines such as TNF- $\alpha$  and TGF- $\beta$  and fibrosis of kidney tissues in the CKD model. (3) Exocue reduced gene expression of miRNAs related to CKD severity and increased levels of AQP2 and AQP5, whereas it reduced BUN and creatinine levels, indicating improved kidney function. Taken together, these results indicate that the Exocue controlled inflammation and fibrosis of kidney tissues and improved kidney function, such as water absorption and filtration of wastes from the blood in the CKD mouse model.

Exosomes derived from MSCs have been used as a promising therapy for neurological, musculoskeletal, cardiovascular, and immunological diseases and disorders.<sup>9</sup> MSC-derived exosomes have been shown to inhibit infiltration, migration, and proliferation of T cells in autoimmune uveitis.<sup>12</sup> Exosomes released from the C3H10T1/2 MSC line alleviate liver fibrosis and acute liver injury via miRNA delivery to endothelial cells.<sup>30</sup> Recently, numerous studies have focused on cell engineering to enhance the therapeutic effect of MSC-derived exosomes.<sup>9</sup> Qazi et al.<sup>31</sup> suggested that MSCs produce exosomes with a higher concentration of cytokines and growth factors in a three-dimensional porous scaffold condition than those produced under two-dimensional culture conditions.<sup>31</sup>

Ma et al.<sup>32</sup> loaded miRNA-132 into exosomes of BM MSCs to promote angiogenesis in myocardial infarction through an electroporation method and they exhibited more efficacy on angiogenesis in heart tissues than naïve exosomes did.<sup>32</sup> In this study, we treated AD MSCs with



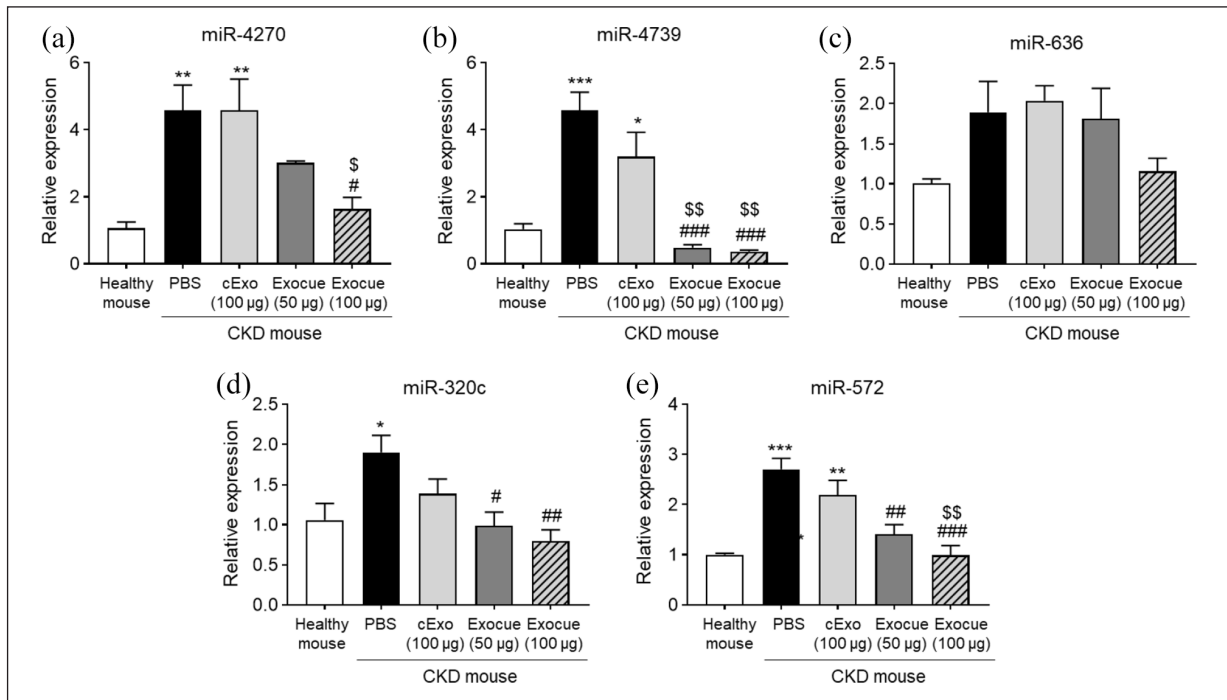


**Figure 6.** Effect of control exomes (cExo), exosomes from melatonin-stimulated mesenchymal stem cells (MSCs, Exocue), and phosphate-buffered saline (PBS) on expression levels of microRNAs (miRNAs) and chronic kidney disease (CKD)-related markers of kidney tissues 3 weeks after injection in CKD mouse model. (a–e) Expression of miR-4270, miR-4739, miR-636, miR-320c, and miR-572 in kidney tissue measured using quantitative reverse transcription-polymerase chain reaction (qRT-PCR). Values represent means  $\pm$  standard error of the means (SEM). \* $p < 0.05$ , \*\* $p < 0.01$ , and \*\*\* $p < 0.001$  versus healthy mice; # $p < 0.05$ , ## $p < 0.01$ , and ### $p < 0.001$  versus PBS; and \$ $p < 0.05$  and \$\$ $p < 0.01$  versus cExo. cExo: control exosome; CKD: chronic kidney disease; Exocue: exosome from melatonin-stimulated MSCs.

melatonin to improve the anti-inflammatory and anti-fibrotic effects of their exosomes in treating CKD. After treatment with melatonin, MSCs secreted exosomes with increased gene expression of *miR-29b-3p*, *miR-7a-3p*, *let-7b-5p*, *let-7c-3p*, *miR-153-3p*, *miR-26a-2-3p*, and *miR-846-5p*, which are related to their anti-inflammatory and anti-fibrosis activity. Furthermore, the exosomes maintained the morphology, size, and EV markers of naïve exosomes. These results indicate that stimulation with melatonin induced MSCs to secrete functionally enhanced exosomes, which maintained their characteristics.

Chronic inflammation and fibrosis of kidney tissues play key roles in the development and progression of CKD and interfere in the major kidney function of ultrafiltration.<sup>33,34</sup> Clinical data showed that patients with CKD had increased circulating levels of inflammatory cytokines such as interleukin-6 and TNF- $\alpha$  and in this study, the serum of mice with CKD also showed higher levels of TNF- $\alpha$  and TGF- $\beta$  than that of healthy mice.<sup>33</sup> High concentrations of cytokines induce the production of other inflammation-related renal cytokines and chemokines, mast cell activation, and facilitate collagen deposition and matrix metalloproteinase (MMP) production, which are crucial fibrosis factors in kidney tissues in CKD.<sup>34</sup> Thus, modulation of the inflammatory conditions of CKD is critical.

The local inflammatory environment could be controlled by MSCs through the regulation of recruitment or polarization of macrophages or both.<sup>6</sup> Exosomes of adipocytes stimulated by melatonin have also been shown to facilitate macrophage phenotype changes from M1 to M2, which is related to anti-inflammatory effects.<sup>35</sup> In this study, Exocue regulated the expression of pro-inflammatory cytokines such as TNF- $\alpha$  and TGF- $\beta$  and these effects might have been induced by its high concentration of miRNA such as *miR-29b-3p*, *miR-7a-3p*, *let-7b-5p*, *let-7c-3p*, *miR-153-3p*, *miR-26a-2-3p*, and *miR-846-5p*, which are known to suppress the TGF- $\beta$  signaling pathway.<sup>36–44</sup> In addition, Exocue also prevented the apoptosis of resident cells, suppressed proliferation of fibroblasts, and decreased  $\alpha$ -SMA and thereby inhibited fibrosis of kidney tissues from the CKD model.

The suppression of TGF- $\beta$  signaling influences the formation of fibrosis in kidney tissues because TGF- $\beta$  modulates the p-Smad2/Smad3 pathway and suppresses collagen, fibronectin, and  $\alpha$ -SMA synthesis.<sup>36–45</sup> Moreover, *miR-29a* suppresses cell proliferation and the expression of collagen I and  $\alpha$ -SMA, which are involved in cardiac fibrosis in rat cardiac fibroblasts.<sup>42</sup> Exosomes derived from MSCs were also found to suppress fibroblast proliferation by downregulating their FZD6 expression via

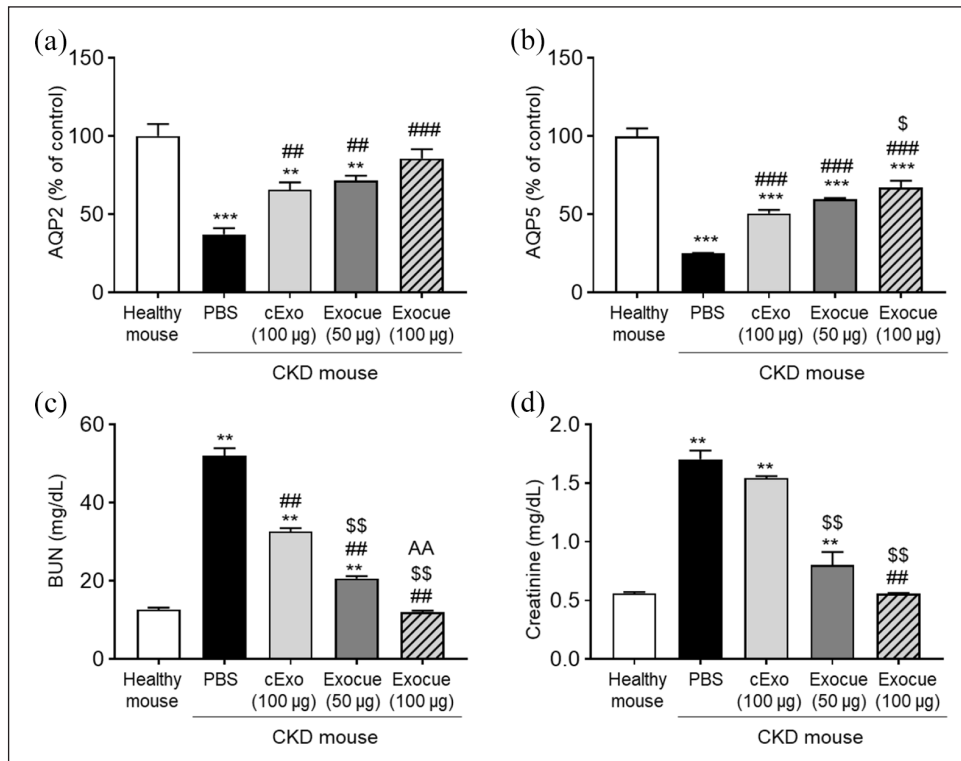


**Figure 7.** Effect of control exomes (cExo), exosomes from melatonin-stimulated mesenchymal stem cells (MSCs, Exocue), and phosphate-buffered saline (PBS) on functional recovery of kidney 3 weeks after injection in chronic kidney disease (CKD) mouse model. (a and b) Concentrations of AQP2 and AQP5 in kidney tissue from CKD mouse model measured using enzyme-linked immunosorbent assay (ELISA). (c and d) Concentrations of BUN and creatinine in serum from CKD mouse model measured using ELISA. Values represent means  $\pm$  standard error of the mean (SEM). \* $p < 0.05$ , \*\* $p < 0.01$ , and \*\*\* $p < 0.001$  versus healthy mice; # $p < 0.05$ , ## $p < 0.01$ , and ### $p < 0.001$  versus PBS; \$ $p < 0.05$  and \$\$ $p < 0.01$  versus cExo; and AA $p < 0.001$  versus Exocue (50  $\mu$ g). AQP2: aquaporin 2; AQP5: aquaporin 5; BUN: blood urea nitrogen; cExo: control exosomes; CKD: chronic kidney disease; Exocue: exosomes from melatonin-stimulated MSCs.

miRNA-29-3p in idiopathic pulmonary fibrosis disease.<sup>43</sup> Therefore, our findings suggest that the suppressive effects of Exocue on inflammation and fibrosis of kidney tissues were probably mediated by the high concentration of miRNAs, which are related to the TGF- $\beta$  signaling pathway. Additionally, it has been reported that exosomes have stable and abundant circRNAs which mediate multiple signaling pathway and the circRNAs act as a sponge of microRNAs.<sup>46–48</sup> Thus, we suggested that CKD related miRNAs, in this study, might be downregulated by circRNAs in exosomes. Of course, further study is needed to reveal the relationship between circRNAs and miRNAs and the healing mechanisms of CKD.

Kidney malfunction of a patient with CKD disrupts homeostasis. Moreover, CKD has been implicated as a primary cause of morbidity and mortality worldwide.<sup>2</sup> Glomerulosclerosis, interstitial fibrosis, and inflammation are the main causes of kidney dysfunction and are involved in the pathogenesis and progression of CKD to end stage renal disease.<sup>45</sup> In particular, dysfunction of the maintenance of body water homeostasis leads to various clinical conditions associated with water balance disorder and

different AQPs play a role in water reabsorption to regulate urine concentration and dilution.<sup>28</sup> Loss of AQP2 function induces a severe defect in urinary concentration.<sup>49</sup> AQP5, the closest homolog to AQP2, is a pivotal protein involved in inflammation.<sup>50</sup> In this study, Exocue increased the expression of AQP2 and AQP5, resulting in the reduction of serum BUN and creatinine levels of CKD mouse. These results indicate that Exocue improved water absorption and waste filtration, which are the main functions of the kidney in a CKD mouse model. Taken together, our findings suggest that Exocue could improve kidney function in CKD through the maintenance of water homeostasis.

## Conclusion

This study demonstrated that Exocue could improve the kidney function by modulating inflammation and fibrosis of the kidney in a CKD mouse model, which may be mediated through upregulation of miRNA expression (Figure 8). We suggest that Exocue might be a one of potential cell-free therapies to improve kidney function and prevent disease progression in patients with CKD.

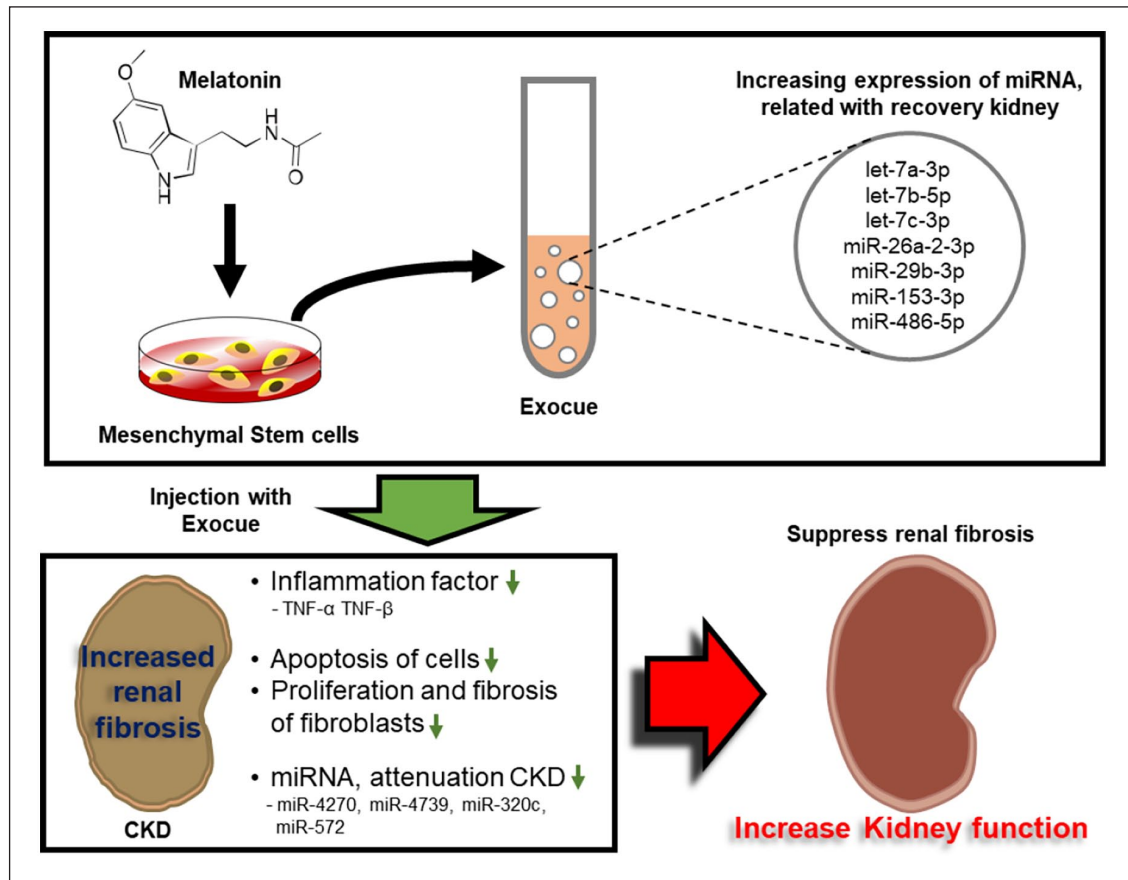


**Figure 8.** Schematic representation of proposed mechanisms by which exosomes from melatonin-stimulated mesenchymal stem cells (MSCs, Exocue) induce functional recovery of kidney in chronic kidney disease (CKD) mouse model. Treatment with melatonin induces MSCs to secrete Exocue containing high concentrations of miRNAs, which are related to kidney recovery. Exocue treatment suppresses inflammatory factors and inhibits apoptosis, proliferation, and interstitial fibrosis of cells in fibrotic kidney tissues. These changes induced by Exocue promotes kidney function.

## Acknowledgements

We thank Jun Hee Lee.

## Author contributions

Ji-Hye Yea, Yeo Min Yoon, Jun Hee Lee, and Chul Won Yun analyzed and interpreted the data and wrote the manuscript. Sang Hun Lee conceived and designed the study, analyzed and interpreted the data, and edited the manuscript.

## Declaration of conflicting interests

The author(s) declared no potential conflicts of interest with respect to the research, authorship, and/or publication of this article.

## Funding

The author(s) disclosed receipt of the following financial support for the research, authorship, and/or publication of this article: This study was supported by a National Research Foundation grant funded by the Korean government (2019M3A9H110349513). The funders had no role in the design of the study, data collection and analysis, decision to publish, or preparation of the manuscript.

## Ethical approval

All animal procedures were conducted in accordance with the protocol approved by the Institutional Animal Care and Use Committee of Soonchunhyang University Seoul Hospital (IACUC-SCH-2020-08).

## ORCID iD

Ji-Hye Yea  <https://orcid.org/0000-0003-0009-2905>

## Availability of data and materials

Data and materials are available upon written request to the corresponding author.

## References

1. Jha V, Garcia-Garcia G, Iseki K, et al. Chronic kidney disease: global dimension and perspectives. *Lancet* 2013; 382: 260–272.
2. Ayodele OE and Alebiosu CO. Burden of chronic kidney disease: an international perspective. *Adv Chronic Kidney Dis* 2010; 17: 215–224.

3. Yoon YM, Lee JH, Song KH, et al. Melatonin-stimulated exosomes enhance the regenerative potential of chronic kidney disease-derived mesenchymal stem/stromal cells via cellular prion proteins. *J Pineal Res* 2020; 68: e12632.
4. Yea J-H, Park J-K, Kim IJ, et al. Regeneration of a full-thickness defect of rotator cuff tendon with freshly thawed umbilical cord-derived mesenchymal stem cells in a rat model. *Stem Cell Res Ther* 2020; 11(1): 387.
5. De Miguel MP, Fuentes-Julian S, Blazquez-Martinez A, et al. Immunosuppressive properties of mesenchymal stem cells: advances and applications. *Curr Mol Med* 2012; 12(5): 574–591.
6. Yea J-H, Bae TS, Kim BJ, et al. Regeneration of tendon-to-bone interface of rotator cuff with umbilical cord derived mesenchymal stem cells and gradient extracellular matrix scaffolds from adipose tissue in a rat model. *Acta Biomater* 2020; 114: 104–116.
7. Yea JH, Kim I, Sym G, et al. Regeneration of a full-thickness defect in rotator cuff tendon with umbilical cord-derived mesenchymal stem cells in a rat model. *PLoS One* 2020; 15: e0235239.
8. Hsieh CF, Alberton P, Loffredo-Verde E, et al. Scaffold-free Scleraxis-programmed tendon progenitors aid in significantly enhanced repair of full-size Achilles tendon rupture. *Nanomed* 2016; 11: 1153–1167.
9. Phan J, Kumar P, Hao D, et al. Engineering mesenchymal stem cells to improve their exosome efficacy and yield for cell-free therapy. *J Extracell Vesicles* 2018; 7: 1522236.
10. Théry C, Ostrowski M and Segura E. Membrane vesicles as conveyors of immune responses. *Nat Rev Immunol* 2009; 9: 581–593.
11. Di Trapani M, Bassi G, Midolo M, et al. Differential and transferable modulatory effects of mesenchymal stromal cell-derived extracellular vesicles on T, B and NK cell functions. *Sci Rep* 2016; 6: 24120.
12. Bai L, Shao H, Wang H, et al. Author correction: effects of mesenchymal stem cell-derived exosomes on experimental autoimmune uveitis. *Sci Rep* 2018; 8: 9889.
13. Kao CY and Papoutsakis ET. Extracellular vesicles: exosomes, microparticles, their parts, and their targets to enable their biomanufacturing and clinical applications. *Curr Opin Biotechnol* 2019; 60: 89–98.
14. Yan Y, Jiang W, Tan Y, et al. hucMSC exosome-derived GPX1 is required for the recovery of hepatic oxidant injury. *Mol Ther* 2017; 25: 465–479.
15. Vader P, Mol EA, Pasterkamp G, et al. Extracellular vesicles for drug delivery. *Adv Drug Deliv Rev* 2016; 106: 148–156.
16. Bei HP, Hung PM, Yeung HL, et al. Bone-a-petite: engineering exosomes towards bone, osteochondral, and cartilage repair. *Small* 2021; e2101741.
17. García JJ, López-Pingarrón L, Almeida-Souza P, et al. Protective effects of melatonin in reducing oxidative stress and in preserving the fluidity of biological membranes: a review. *J Pineal Res* 2014; 56: 225–237.
18. Reiter RJ. Pineal melatonin: cell biology of its synthesis and of its physiological interactions. *Endocr Rev* 1991; 12: 151–180.
19. Han YS, Yoon YM, Go G, et al. Melatonin protects human renal proximal tubule epithelial cells against high glucose-mediated fibrosis via the cellular prion protein-TGF- $\beta$ -smad signaling axis. *Int J Med Sci* 2020; 17: 1235–1245.
20. Chen YT, Chuang FC, Yang CC, et al. Combined melatonin-adipose derived mesenchymal stem cells therapy effectively protected the testis from testicular torsion-induced ischemia-reperfusion injury. *Stem Cell Res Ther* 2021; 12: 370.
21. Mias C, Trouche E, Seguelas MH, et al. Ex vivo pretreatment with melatonin improves survival, proangiogenic/mitogenic activity, and efficiency of mesenchymal stem cells injected into ischemic kidney. *Stem Cells* 2008; 26: 1749–1757.
22. Han D, Huang W, Li X, et al. Melatonin facilitates adipose-derived mesenchymal stem cells to repair the murine infarcted heart via the SIRT1 signaling pathway. *J Pineal Res* 2016; 60: 178–192.
23. Zhu P, Liu J, Shi J, et al. Melatonin protects ADSCs from ROS and enhances their therapeutic potency in a rat model of myocardial infarction. *J Cell Mol Med* 2015; 19: 2232–2243.
24. Yip HK, Chang YC, Wallace CG, et al. Melatonin treatment improves adipose-derived mesenchymal stem cell therapy for acute lung ischemia-reperfusion injury. *J Pineal Res* 2013; 54(2): 207–221.
25. Lee JH, Han YS and Lee SH. Melatonin-induced PGC-1 $\alpha$  improves angiogenic potential of mesenchymal stem cells in hindlimb ischemia. *Biomol Ther* 2020; 28: 240–249.
26. Lv C, Kong H, Dong G, et al. Antitumor efficacy of  $\alpha$ -solanine against pancreatic cancer in vitro and in vivo. *PLoS One* 2014; 9: e87868.
27. Thongboonkerd V. Roles for exosome in various kidney diseases and disorders. *Front Pharmacol* 2019; 10: 1655.
28. Su W, Cao R, Zhang X-Y, et al. Aquaporins in the kidney: physiology and pathophysiology. *Am J Physiol Renal Physiol* 2020; 318: F193–F203.
29. de Braganca AC, Moyses ZP and Magaldi AJ. Carbamazepine can induce kidney water absorption by increasing aquaporin 2 expression. *Nephrol Dial Transplant* 2010; 25: 3840–3845.
30. Gong M, Yu B, Wang J, et al. Mesenchymal stem cells release exosomes that transfer miRNAs to endothelial cells and promote angiogenesis. *Oncotarget* 2017; 8: 45200–45212.
31. Qazi TH, Mooney DJ, Duda GN, et al. Biomaterials that promote cell-cell interactions enhance the paracrine function of MSCs. *Biomaterials* 2017; 140: 103–114.
32. Ma T, Chen Y, Chen Y, et al. MicroRNA-132, delivered by mesenchymal stem cell-derived exosomes, promote angiogenesis in myocardial infarction. *Stem Cells Int* 2018; 2018: 3290372.
33. Stenvinkel P, Wanner C, Metzger T, et al. Inflammation and outcome in end-stage renal failure: does female gender constitute a survival advantage? *Kidney Int* 2002; 62: 1791–1798.
34. Impellizzeri D, Esposito E, Attley J, et al. Targeting inflammation: new therapeutic approaches in chronic kidney disease (CKD). *Pharmacol Res* 2014; 81: 91–102.
35. Liu Z, Gan L, Zhang T, et al. Melatonin alleviates adipose inflammation through elevating  $\alpha$ -ketoglutarate and diverting

- adipose-derived exosomes to macrophages in mice. *J Pineal Res* 2018; 64: e12455.
36. Brennan EP, Nolan KA, Börgeson E, et al. Lipoxins attenuate renal fibrosis by inducing let-7c and suppressing TGF $\beta$ R1. *J Am Soc Nephrol* 2013; 24: 627–637.
  37. Ji X, Wu B, Fan J, et al. The anti-fibrotic effects and mechanisms of MicroRNA-486-5p in pulmonary fibrosis. *Sci Rep* 2015; 5: 14131.
  38. Jiang XP, Ai WB, Wan LY, et al. The roles of microRNA families in hepatic fibrosis. *Cell Biosci* 2017; 7: 34.
  39. Liang C, Li X, Zhang L, et al. The anti-fibrotic effects of microRNA-153 by targeting TGFBR-2 in pulmonary fibrosis. *Exp Mol Pathol* 2015; 99: 279–285.
  40. Liang H, Xu C, Pan Z, et al. The antifibrotic effects and mechanisms of microRNA-26a action in idiopathic pulmonary fibrosis. *Mol Ther* 2014; 22: 1122–1133.
  41. Lv W, Fan F, Wang Y, et al. Therapeutic potential of microRNAs for the treatment of renal fibrosis and CKD. *Physiol Genomics* 2018; 50: 20–34.
  42. Qin RH, Tao H, Ni SH, et al. MicroRNA-29a inhibits cardiac fibrosis in Sprague-Dawley rats by downregulating the expression of DNMT3A. *Anatol J Cardiol* 2018; 20: 198–205.
  43. Wan X, Chen S, Fang Y, et al. Mesenchymal stem cell-derived extracellular vesicles suppress the fibroblast proliferation by downregulating FZD6 expression in fibroblasts via microRNA-29b-3p in idiopathic pulmonary fibrosis. *J Cell Physiol* 2020; 235: 8613–8625.
  44. Zhang Y, Guo J, Li Y, et al. let-7a. *Exp Ther Med* 2019; 17: 3935–3942.
  45. Chen L, Yang T, Lu DW, et al. Central role of dysregulation of TGF- $\beta$ /smad in CKD progression and potential targets of its treatment. *Biomed Pharmacother* 2018; 101: 670–681.
  46. Wang Y, Liu J, Ma J, et al. Exosomal circRNAs: biogenesis, effect and application in human diseases. *Mol Cancer* 2019; 18(1): 116.
  47. Wang R, Zhang S, Chen X, et al. CircNT5E acts as a sponge of miR-422a to promote glioblastoma tumorigenesis. *Cancer Res* 2018; 78: 4812–4825.
  48. Granados-Riveron JT and Aquino-Jarquin G. The complexity of the translation ability of circRNAs. *Biochim Biophys Acta* 2016; 1859: 1245–1251.
  49. Rojek A, Füchtbauer E-M, Kwon T-H, et al. Severe urinary concentrating defect in renal collecting duct-selective AQP2 conditional-knockout mice. *Proc Natl Acad Sci USA* 2006; 103: 6037–6042.
  50. Rump K, Unterberg M, Bergmann L, et al. AQP5-1364A/C polymorphism and the AQP5 expression influence sepsis survival and immune cell migration: a prospective laboratory and patient study. *J Transl Med* 2016; 14(1): 321.